

## SEEING THE COLLISION OF A SUPERNOVA WITH ITS COMPANION STAR

DANIEL KASEN<sup>1,2</sup>

*Draft version October 31, 2018*

### ABSTRACT

The progenitors of Type Ia and some core collapse supernovae are thought to be stars in binary systems, but little observational evidence exists to confirm the hypothesis. We suggest that the collision of the supernova ejecta with its companion star should produce detectable emission in the hours and days following the explosion. The interaction occurs at distances  $\sim 10^{11} - 10^{13}$  cm and shocks the impacting supernova debris, dissipating kinetic energy and re-heating the gas. Initially, some radiation may escape promptly through the evacuated region of the shadowcone, producing a bright X-ray (0.1-2 keV) burst lasting minutes to hours with luminosity  $L \sim 10^{44}$  ergs s<sup>-1</sup>. Continuing radiative diffusion from deeper layers of shock heated ejecta produces a longer lasting optical/UV emission which exceeds the radioactively powered luminosity of the supernova for the first few days after the explosion. These signatures are prominent for viewing angles looking down upon the shocked region, or about 10% of the time. The properties of the emission provide a straightforward measure of the separation distance between the stars and hence (assuming Roche lobe overflow) the companion's radius. Current optical and UV data sets likely already constrain red giant companions. By systematically acquiring early time data for many supernovae, it should eventually be possible to empirically determine how the parameters of the progenitor system influence the outcome of the explosion.

*Subject headings:*

### 1. INTRODUCTION

Observations of supernova light curves and spectra have allowed us to characterize the outcome of the explosion – the burned and ejected stellar debris – in remarkable detail. But we still know very little about the starting point. In the most widely considered scenario, Type Ia supernovae (SNe Ia) result from carbon/oxygen white dwarfs which reach a critical mass by accreting material from a non-degenerate companion star. Observational confirmation of the binary nature of the progenitor system is lacking, however, and almost nothing is known about the properties and diversity of the companion stars. The proposed progenitors should be rather dim, so it is not surprising that we have so far failed to find them in pre-explosion images of the host galaxies (e.g., Maoz & Mannucci 2008). One therefore seeks other means of inferring the presence of a stellar companion.

A few minutes to hours after the supernova eruption, the debris ejected in the explosion is expected to overrun the companion. The star is shocked by the impact, and its envelope partially stripped and ablated, but it survives the ordeal (Wheeler et al. 1975; Fryxell & Arnett 1981; Chugai 1986; Livne et al. 1992; Marietta et al. 2000; Pakmor et al. 2008). Observations of the remnant of Tycho's 1572 supernova turned up a high-velocity G star, claimed to be the runaway companion (Ruiz-Lapuente et al. 2004). This identification is still debated (Kerzendorf et al. 2009). Meanwhile, several attempts to look for evidence of stripped hydrogen in the spectra of SNe Ia have detected nothing (Mattila et al. 2005; Leonard 2007). The supernova ejecta is distorted by the collision, which should lead to polarization of the supernova light (Kasen et al. 2004). But although polarization

has been detected in several SNe Ia (Wang & Wheeler 2008), there is nothing to unambiguously indicate that this asymmetry relates to companion interaction.

While the previous investigations have focused on the long term consequences, one might wonder: could we see the collision itself? Here we can draw an interesting parallel with core collapse supernova explosions, in which a shock wave propagates through the envelope of a massive star. When that shock front nears the stellar surface at radius  $R \approx 10^{11} - 10^{13}$  cm, the post shock energy vents in an X-ray breakout burst lasting minutes to hours (Klein & Chevalier 1978; Matzner & McKee 1999). In the days that follow, optical/UV radiation continues to diffuse from the deeper layers of shock heated ejecta. Eventually, the energy deposition from radioactive <sup>56</sup>Ni decay takes over. The early shock luminosity phase, however, has been observed in several events, e.g., SN 1987A (Arnett et al. 1989) and SN 1993J (Wheeler et al. 1993) while the shock breakout itself was caught for SN 2008D (Soderberg et al. 2008; Modjaz et al. 2009).

The same physics applies to Type Ia supernovae, but because the radius of the progenitor white dwarf is so small ( $R_{\text{wd}} \approx 2 \times 10^8$  cm) the breakout emission should be extremely brief and the early luminosity remarkably dim. The problem is that when energy input occurs at small radii, adiabatic losses in the rapidly expanding ( $v \approx 10^9$  cm s<sup>-1</sup>) ejecta are overwhelming, and the thermal shock deposited energy is converted to kinetic energy on the expansion timescale ( $R_{\text{wd}}/v \sim 0.1$  sec), which is much shorter than the diffusion timescale.

As it turns out, the separation distance between the white dwarf and its companion star is presumed to be  $a \sim 10^{11} - 10^{13}$  cm, comparable to the radii of core collapse progenitors. When the supernova ejecta collides with its companion, the impacting layers are re-shocked and the kinetic energy partially dissipated. If the geometry is

<sup>1</sup> University of California, Santa Cruz

<sup>2</sup> Hubble Fellow

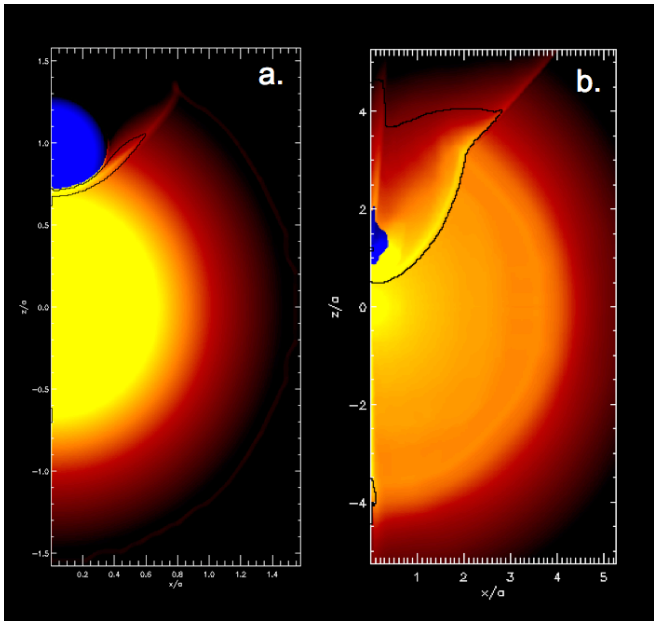


FIG. 1.— Hydrodynamical calculation of a Type Ia supernova colliding with a red giant star ( $R_\star = 10^{13}$  cm,  $a = 2.5 \times 10^{13}$  cm). **a:** Density structure during the prompt emission phase ( $t = t_i/2$ ). The companion star (drawn in blue) diverts the flow and carves a hole in the ejecta. The black contour shows the region where the shocked ejecta temperature exceeds  $3 \times 10^5$  K. **b:** Density structure at a later phase ( $t = 2t_i$ , note change of scale). The shell of shocked ejecta has expanded to partially refill the hole. The black contour shows the region where the temperature exceeds  $10^5$  K.

favorable, some of this energy might escape straightaway in a prompt burst, which will be followed by a longer-lasting tail of diffusive emission – the analogues of shock breakout and its aftermath in core collapse events. In this case the emission provides a measure not of the stellar radius  $R_{\text{wd}}$ , but of the separation distance  $a$ .

Here we develop an analytic description of the collision dynamics and subsequent radiation transport which suggests that early time observations of supernovae at X-ray through optical wavelengths should offer a powerful means of confirming the presence of a companion star and constraining its parameters.

## 2. COLLISION DYNAMICS

In the single degenerate scenario of SNe Ia, the companion stars are thought to be either slightly evolved main sequence stars or red giants (Branch et al. 1995; Hachisu et al. 1996). For the most promptly exploding systems, the companions may be 5–6  $M_\odot$  main sequence (MS) sub-giants, with radii  $R_\star \sim 5 \times 10^{11}$  cm. More commonly, the MS companions may be 1–3  $M_\odot$  sub-giants with radii  $\sim 1 - 3 \times 10^{11}$  cm. In the red giant (RG) case, the stars are evolved  $\sim 1 - 2 M_\odot$  stars with  $R_\star \sim 10^{13}$  cm. In most scenarios, the companion is believed to be in Roche lobe overflow. The separation distance,  $a$ , is then comparable to the companion radius; for typical mass ratios,  $a/R_\star = 2 - 3$ .

After the supernova explodes, the ejected debris expands freely for some time before hitting the companion. The flow becomes homologous, and the radius of a fluid element  $r = vt$  where  $v$  is the velocity and  $t$  is the time since explosion. We will describe the ejecta density profile by a broken power law (Chevalier & Soker 1989) with

a shallow inner region  $\rho_i \propto r^{-\delta}$  and a steep outer region  $\rho_o \propto r^{-n}$ . The profiles join at the transition velocity

$$v_t = 6 \times 10^8 \zeta_v (E_{51}/M_c)^{1/2} \text{ cm s}^{-1}, \quad (1)$$

where  $E_{51} = E/10^{51}$  ergs is the explosion energy,  $M_c = M/M_{\text{ch}}$  is the ejecta mass in units of the Chandrasekhar mass, and  $\zeta_v$  is a numerical constant. The density in the outer layers ( $v > v_t$ ) is

$$\rho_o(r, t) = \zeta_\rho \frac{M}{v_t^3 t^3} \left( \frac{r}{v_t t} \right)^{-n} \quad (2)$$

with a similar expression for the inner layers. The numerical constants follow from the requirement that the density integrate to the specified mass and kinetic energy

$$\zeta_v = \left[ \frac{2(5-\delta)(n-5)}{(3-\delta)(n-3)} \right]^{1/2} \quad (3)$$

$$\zeta_\rho = \frac{1}{4\pi} \frac{(n-3)(3-\delta)}{n-\delta}.$$

The broken power law profile was originally derived for core collapse supernovae, but it fits multi-dimensional delayed-detonation models of SNe Ia remarkably well. For the models of Kasen et al. (2009) we find typical values of  $\delta = 1$ ,  $n = 10$ , in which case the constants are  $\zeta_v = 1.69$ ,  $\zeta_\rho = 0.12$ .

The characteristic timescale for the supernova ejecta to interact with the companion is

$$t_i = a/v_t = 10^4 a_{13} v_9^{-1} \text{ sec}, \quad (4)$$

where  $a_{13} = a/10^{13}$  cm, and  $v_9 = v_t/10^9$  cm s $^{-1}$ . For RG companions the interaction timescale  $t_i \approx 5$  hours, while for MS sub-giants,  $t_i \approx 5 - 30$  minutes.

The ejecta is highly supersonic when it collides with the companion, with mach number  $\mathcal{M} \approx (a/R_{\text{wd}})^{1/2} \gg 1$ . Figure 1 illustrates the hydrodynamics of the interaction in a 2-dimensional numerical calculation using the FLASH code (Fryxell et al. 2000) and assuming a polytropic  $\gamma = 4/3$  equation of state, appropriate for a radiation dominated gas. As the flow sweeps over the companion star, a bow shock forms. Ejecta passing through the shock is heated and compressed into a thin shell, and its velocity vector is redirected.

We will rely here on an approximate analytic description of the collision dynamics. Material moving at velocity  $v$  interacts at a time  $t_v \approx a/v$ . The ejecta properties immediately after being shocked are given by the Rankine-Hugoniot jump conditions in the hypersonic limit. The density of the shocked gas is

$$\rho_s(v) = \frac{\gamma+1}{\gamma-1} \rho_0(a, t_v) = 7\zeta_\rho \frac{M}{a^3} \left( \frac{v}{v_t} \right)^{-n+3} \quad (5)$$

taking  $\gamma = 4/3$ . The pressure of the shocked gas is of order the incoming ram pressure

$$p_s(v) = \frac{2}{1+\gamma} \rho_0 v^2 \sin^2 \chi = \frac{6}{7} \zeta_\rho \sin^2 \chi \frac{M v_t^2}{a^3} \left( \frac{v}{v_t} \right)^{-n+5} \quad (6)$$

where  $\chi$  is the angle of the oblique shock front relative to the flow direction. The actual value of  $\chi$  varies along the bow shock, but for simplicity we take a constant,

characteristic value near the maximal turning angle for hypersonic flows,  $\chi \approx 45^\circ$ .

For a radiation dominated gas,  $p_s = a_R T_s^4/3$ , where  $a_R$  is the radiation constant, which gives the equilibrium temperature of the shocked debris

$$T_s(v) = 2.8 \times 10^6 M_c^{1/4} v_9^{1/2} a_{13}^{-3/4} \left(\frac{v}{v_t}\right)^{-(n-5)/4} \text{ K} \quad (7)$$

For a RG companion at  $a = 2.5 \times 10^{13}$  cm, the outer layers of ejecta ( $v \sim 3v_t$ ) have  $T_s \approx 3 \times 10^5$  K, a value confirmed by the numerical calculation (Figure 1a). MS companions will have higher shock temperatures with  $T_s \approx 10^6 - 10^7$  K. To check the assumption of radiation domination in the shocked region, we note that Eqs. 5 and 6 imply a ratio of radiation energy to electron/ion energy

$$\frac{aT_s^4}{\rho_s k_B T_s / m_p} = 707 a_{13}^{3/4} M_c^{-1/4} v_9^{3/2} \quad (8)$$

which is  $\gg 1$  for the scenarios under consideration. The details of thermalization, however, deserve further investigation. Initially, the electrons/ions are shocked to very high temperatures ( $\sim 10^9 - 10^{10}$  K), then radiatively cool toward the equilibrium value Eq. 7 by processes similar to those in ordinary supernova shocks – i.e., bremsstrahlung followed by Compton up-scattering, and in some cases pair-production (Weaver 1976). If the timescale for the gas to radiate lags the dynamical timescale, non-equilibrium temperatures significantly greater than  $T_s$  can be realized in the relaxation region. This is likely to occur in the highest-velocity, lowest-density outermost layers, and may be a source of harder radiation (Katz et al. 2009).

The interaction with the companion diverts the incoming flow, carving out a conical hole in the supernova ejecta. The half opening angle of the hole is roughly  $\theta_h = \tan^{-1}(r_b/a)$  where  $r_b$  is the extent of the bow shock. Simulations find  $r_b \sim 2R_*$  and  $\theta_h = 30 - 40^\circ$  (see Figure 1 and Marietta et al. (2000)). The solid angle,  $\Omega_h$ , of the hole is

$$\frac{\Omega_h}{4\pi} = \frac{1}{2}(1 - \cos \theta_h) = \frac{1}{2} \left[ 1 - \frac{1}{1 + (r_b/a)^2} \right] \approx \frac{1}{10} \quad (9)$$

This hole will provide a channel for radiation to quickly escape from the otherwise optically thick ejecta.

The ejecta displaced from the hole piles up into a compressed shell along the cone surface. Assuming this shell layer is thin, its thickness  $l_{sh}$  can be estimated by mass conservation. The volume of a region of radial extent  $dr$  within the conical cavity is  $V_i = \Omega_h a^2 dr$ . The gas swept out of this region occupies a volume  $V_f = 2\pi a l_{sh} dr$ . The condition  $\rho_0 V_i = \rho_s V_f$  gives

$$\frac{l_{sh}}{a} = \frac{\Omega_h 2\rho_0}{4\pi \rho_s} \approx \frac{1}{35} \quad (10)$$

A dense shell of roughly this thickness is seen in Figure 1a. The actual dynamics can become quite complex, with the shell broken in pieces by shear instabilities and the companion envelope shredded.

After passing by the companion star, the shocked gas can expand laterally to try to refill the evacuated hole.

The situation resembles the isentropic expansion of a gas cloud into vacuum (Zel'Dovich & Raizer 1967); the front of the rarefaction wave moves outward at the maximum escape velocity  $v_l = 2/(\gamma-1)c_s$  where  $c_s = (\gamma p_s/\rho_s)^{1/2} = (8/49)^{1/2} \sin \chi v$  is the sound speed of the shocked material. The net velocity in the direction perpendicular to the symmetry axis is then  $v_x = v \sin \theta_h - v_l \cos \theta_h \approx -0.2 v$ . The ejecta moving at velocity  $v$  thus re-closes at a time  $R_*/|v_x| \approx 5R_*/v$  after passing by the companion, or at a time  $t_h = (a + 6R_*)/v$  after the explosion. In the adiabatic calculation (Figure 1b), the rarefaction softens the density gradient in the polar direction, but fails to refill the shadowcone region uniformly before freezing out. If radiative cooling is significant during these phases (see Section 3) the sound speed will be reduced, which would further delay or halt the closing of the hole.

The energy density of the shocked gas is  $\epsilon_s = 3p_s$  and so the total energy dissipated in the collision shock is found to be

$$E_{th} = \frac{18}{49} \sin^2 \chi \frac{\Omega_h}{4\pi} E \approx 1.5 \times 10^{49} E_{51} \text{ ergs.} \quad (11)$$

Much of this thermal energy will be lost again to adiabatic expansion, but if even a fraction is radiated the collision luminosity should be quite bright.

### 3. PROMPT X-RAY BURST

As supernova ejecta flows past the companion star, the hot surface layers of the shocked shell become exposed (Figure 1a). At this time, some radiation may be able to escape straightaway through the evacuated shadowcone hole, giving rise to a sudden burst of emission. In general, only a fraction of the total energy in the shell can be radiated promptly – i.e., before suffering significant losses due to adiabatic expansion. This prompt emission arises from the surface layer of the shell with a thickness,  $l_d$ , determined by requiring that the diffusion time through that layer

$$t_d = \tau \frac{l_d}{3c} = \frac{l_d^2 \kappa \rho_s}{3c} \quad (12)$$

be less than the timescale for expansion, given by the shell sound crossing time  $l_{sh}/c_s$  (which is typically shorter than the dynamical timescale  $a/v$ ). Using Eqs. 5 and 10 gives

$$\frac{l_d}{l_{sh}} = \frac{a}{v_t t_{sn}} \left(\frac{4\pi}{\Omega_h}\right)^{1/2} \left(\frac{\sqrt{8}}{14\zeta_\rho \sin \chi}\right)^{1/2} \left[\frac{v}{v_t}\right]^{(n-4)/2} \quad (13)$$

where the quantity

$$t_{sn} = \left(\frac{\kappa M}{3c v_t}\right)^{1/2} = 29 M_c^{1/2} v_9^{-1/2} \kappa_e^{1/2} \text{ days} \quad (14)$$

is the familiar "effective" diffusion time (Arnett 1982) that sets the duration of the ordinary  $^{56}\text{Ni}$ -powered SN Ia light curve. We have assumed a constant opacity  $\kappa_e = 0.2 \text{ cm}^2 \text{g}^{-1}$ , appropriate for electron scattering in fully ionized  $A/Z = 2$  elements. For RG companions at  $a \approx 10^{13}$  cm, we find  $l_d \simeq l_{sh}$  for the layers  $v \gtrsim 2v_t$ . In this case, most of the energy dissipated in the outer layers can be radiated in the prompt burst. For MS companions with  $a \simeq 10^{11} - 10^{12}$  cm, the ratio  $l_d/l_{sh} \simeq 0.01 - 0.1$ , and only a fraction of the photons escape promptly.

While the bulk of the SN ejecta remains extremely optically thick at this phase, photons can initially escape through the hole carved out in the interaction. This channel will close, however, once the outer layers of ejecta have re-expanded to fill the shadowcone, which happens at a time  $t_h \approx (a + 6R_*)/v_{\max}$  where  $v_{\max}$  is the maximum ejecta velocity (see Section 2). A given layer of ejecta can contribute to the burst only if it passes the companion at a time less than  $t_h$ , which holds for material moving faster than  $v_{\min} \approx v_{\max}(a + R_*)/(a + 6R_*)$ . For  $a/R_* = 3$ , we find  $v_{\min} \approx v_{\max}/2$ .

By integrating the energy density,  $\epsilon_s = 3p_s$ , of the shocked gas within  $l_d$ , we can estimate the total energy escaping in the burst

$$\begin{aligned} E_x &= 2\pi \int_{v_{\min}}^{v_{\max}} 3p_s(v)l_d(v) a \left(\frac{a}{v}\right) dv \\ &= 7.72 \times 10^{47} \left(\frac{\Omega_h}{4\pi}\zeta_\rho \sin^3 \chi\right)^{1/2} \left(\frac{62}{n-6}\right) \times \\ &\quad a_{13}M_c^{1/2}v_9^{3/2}\kappa_e^{-1/2} \left(\frac{v_t}{v_{\min}}\right)^{(n-6)/2} \text{ ergs,} \end{aligned} \quad (15)$$

where we approximated the upper limit as  $v_{\max} \rightarrow \infty$ . The duration of the burst is the time it takes the emitting ejecta to flow past the companion, or  $\Delta t_x = (a + R_*)/v_{\min} - (a + R_*)/v_{\max}$ . For typical values ( $v_{\min} \approx 2v_t$ ;  $v_{\max} \approx 4v_t$ ;  $R_* \approx 3a$ ) this duration is  $\Delta t_x \approx t_i/3$ . Assuming the radiation is emitted into a solid angle  $\Omega_h$ , the isotropic equivalent luminosity is  $L_{x,\text{iso}} = (4\pi/\Omega_h)(E_x/\Delta t_x)$ . Taking characteristic values  $(n, \delta, \chi, \theta_h, v_{\min}) = (10, 1, 45^\circ, 40^\circ, 2v_t)$  we find

$$L_{x,\text{iso}} = 5.8 \times 10^{44} M_c^{1/2}v_9^{5/2}\kappa_e^{-1/2} \text{ ergs s}^{-1} \quad (16)$$

This luminosity is independent of  $a$ , and so roughly comparable for all types of companions. The value is similar to that of shock breakout in core collapse SNe, which is not surprising given that the shock temperature and emitting surface area are comparable in the two phenomena. The collision burst will only be visible for viewing angles peering down the hole,  $\theta \lesssim \theta_h$ . Such an orientation occurs  $\Omega_h/4\pi \approx 10\%$  of the time.

The spectrum of the prompt burst may be approximated as a blackbody at the equilibrium shock temperature (Eq. 7), implying emission peaking in the soft X-ray with typical energies  $T_x \sim 0.05 - 0.1$  keV for RG and  $T_x \sim 0.2 - 2$  keV for MS companions. Non-equilibrium effects (see Section 2) could lead to some emission at significantly higher energies (10 – 100 keV), while non-thermal particle acceleration may also contribute a power law continuum of hard radiation. X-rays emitted in the direction of the companion star will ionize its surface layers and be reprocessed, likely giving rise to substantial line recombination/fluorescence emission (e.g., Balantyne & Ramirez-Ruiz 2001).

According to Eq. 7 the temperature of the burst spectrum evolves with time as

$$T_x(t) = 0.1 a_{13}^{-3/4} M_c^{1/4} v_9^{1/2} \left(\frac{t}{t_i/2}\right)^{(n-5)/4} \text{ keV,} \quad (17)$$

which predicts that, at least initially, the spectrum becomes harder with time, as interior layers of ejecta have

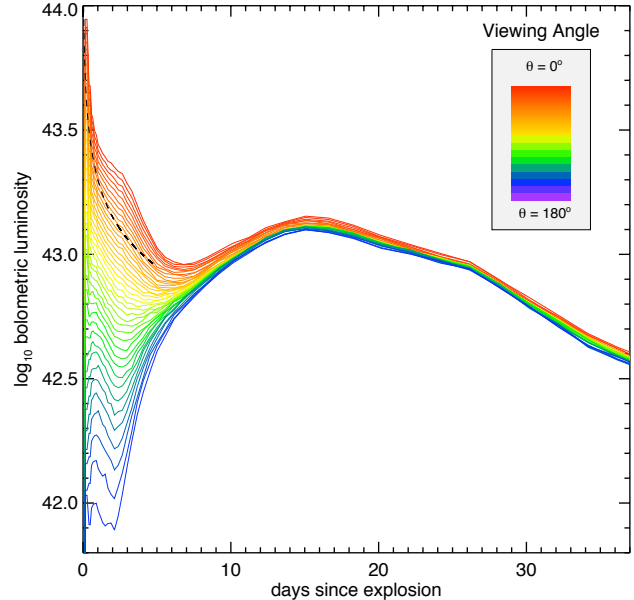


FIG. 2.— Model light curve of a Type Ia supernova having collided with a red giant companion at a separation distance  $a = 2 \times 10^{13}$  cm. The luminosity due to the collision is prominent at times  $t < 8$  days and for viewing angles looking down on the collision region ( $\theta = 0^\circ$ ). At later times the emission is powered by the radioactive decay of  $0.6 M_\odot$  of  $^{56}\text{Ni}$  located in the inner layers of ejecta ( $v < 10^9$  cm s $^{-1}$ ). The black dashed line shows the analytic prediction for the early phase luminosity (Eq. 22).

higher densities and shock temperatures. On the other hand, deviations from equilibrium are likely to be greatest in the highest velocity layers, which may counteract this trend. Eventually, as ejecta gradually refills the shadowcone, the effective photosphere moves to a larger radius and the emission must soften.

The actual structure of the collision region will be more complex and inhomogeneous than that imagined here, due either to the inherent clumpiness of the supernova ejecta, or to secondary shocks and hydrodynamical instabilities developing in the interaction (e.g., Cid-Fernandes et al. 1996). This may lead to fluctuations in the burst light curve on a time scale  $\delta R/v$  where  $\delta R$  is the typical clump size. Multi-dimensional radiation-hydrodynamics calculations will be needed to characterize the light curve and spectra in detail.

#### 4. EARLY UV/OPTICAL LUMINOSITY

Thermal energy not radiated in the prompt burst can diffuse out in the hours and days that follow, but will suffer losses from adiabatic expansion. At  $t \sim 1$  day, this emission will be primarily at UV/optical wavelengths.

We consider here times  $\gg t_i$  such that homology has been re-established in the ejecta. The final ejecta structure will be asymmetric, but for now we neglect angular dependencies. The density profile is taken to be  $\rho_f(r, t) = 7f_0 \rho_0(r, t)$ , where the constant  $f_0 < 1$  accounts for the lateral expansion and radial readjustment that occur during the transition to homology.

Assuming the evolution is adiabatic, the pressure profile of a shocked fluid element at these times is  $p_f(t) = p_s[\rho_f(t)/\rho_s]^\gamma$ . For the region affected by the collision

( $\theta < \theta_h$ )

$$p_f(r, t) = \frac{6}{7} f_0^{4/3} \zeta_\rho \sin^2 \chi \frac{Ma}{v_t^2 t^4} \left( \frac{r}{v_t t} \right)^{-n+1} \quad (18)$$

The pressure is negligible outside  $\theta_h$ . As time progresses, the adiabatic profile Eq. 18 will continue to describe the opaque inner layers of ejecta, but the outer layers will be modified by radiative diffusion. The evolution can be calculated using a self-similar diffusion wave analysis (Chevalier 1992). At a time  $t$ , diffusion will have affected the ejecta above a radius  $r_d$  determined by setting the diffusion time  $t_d = r_d^2 \kappa \rho_f / 3c$  equal to the elapsed time  $t$

$$r_d(t) = \left[ \frac{\zeta_\rho t_{\text{sn}}^2}{3} \right]^{1/(n-2)} v_t t^{(n-4)/(n-2)} \quad (19)$$

Over time, the diffusion wave recedes into the ejecta in a Lagrangian sense. However, for times  $t \lesssim 5$  days,  $r_d$  remains in the steep outer layers of ejecta ( $v > v_t$ ).

Considering only the radial transport, the isotropic equivalent luminosity in the comoving frame is given by the diffusion approximation

$$L_{c,\text{iso}}(r, t) = -4\pi r^2 \frac{c}{\kappa \rho_f} \frac{\partial p_f}{\partial r} \quad (20)$$

We continue to assume a constant opacity, even though at UV wavelengths the line expansion opacity may exceed electron scattering and will, to some extent, be temperature dependent.

In the outer layers of ejecta ( $r > r_d$ ) the comoving luminosity  $L_{c,\text{iso}}$  is constant with radius. Its value is therefore set by processes near the diffusion wave radius. A reasonable estimate of  $L_{c,\text{iso}}$  is derived by evaluating Eq. 20 at  $r_d$ , using the pressure profile Eq. 18,

$$L_{c,\text{iso}} = \frac{16\pi}{49} (n-1) \eta \sin^2 \chi f_0^{1/3} \left[ \frac{\zeta_\rho}{3} \right]^{2/(n-2)} \times \left( \frac{t_i}{t_{\text{sn}}^2} \right) \frac{1}{2} M v_t^2 \left( \frac{t}{t_{\text{sn}}} \right)^{-4/(n-2)} \quad (21)$$

where  $\eta$  is a constant of order unity that must be determined by solving the full diffusion equation (Chevalier 1992). Written in this form, the resemblance to core collapse supernova light curves is clear: apart from constants, the luminosity is of order  $E/t_{\text{sn}}$  times a factor  $t_i/t_{\text{sn}}$  that accounts for adiabatic losses.

Taking  $(n, \delta, \chi, f_0, \eta) = (10, 1, 45^\circ, 0.5, 0.5)$  we find that from appropriate viewing angles

$$L_{c,\text{iso}} = 10^{43} a_{13} M_c^{1/4} v_9^{7/4} \kappa_e^{-3/4} t_{\text{day}}^{-1/2} \text{ ergs s}^{-1}, \quad (22)$$

where  $t_{\text{day}}$  is the time since explosion measured in days. The derivation applies only at times significantly greater than  $t_i$ , but Eq. 22 may provide a workable estimate at earlier times. The observer frame luminosity differs from Eq. 22 by an additional term accounting for the advected luminosity, of order  $v/c \lesssim 10\%$  compared to  $L_{c,\text{iso}}$ .

The collision luminosity will only be readily discernible when it exceeds the luminosity,  $L_{\text{ni}}$ , of the ordinary  $^{56}\text{Ni}$  powered light curve. At early times,  $t \ll t_{\text{sn}}$ , the approximate analytic light curves of SNe Ia give  $L_{\text{ni}} = \epsilon_{\text{ni}} M_{\text{ni}} (t/t_{\text{sn}})^2$ , where  $\epsilon_{\text{ni}} = 4.8 \times 10^{10} \text{ ergs s}^{-1} \text{ g}^{-1}$

and  $M_{\text{ni}}$  is the mass of  $^{56}\text{Ni}$  (Arnett 1982). We then find that  $L_{c,\text{iso}} > L_{\text{ni}}$  for times

$$t_c < 7.3 a_{13}^{2/5} M_c^{1/2} v_9^{3/10} \kappa_e^{1/10} \left( \frac{\kappa_{\text{ni}}}{\kappa_e} \right)^{2/5} M_{\text{ni},0.6}^{-2/5} \text{ days}, \quad (23)$$

where  $M_{\text{ni},0.6} = M_{\text{ni}}/0.6M_\odot$ . Note that the opacity in the  $^{56}\text{Ni}$  region,  $\kappa_{\text{ni}}$ , is heavily affected by iron group line blanketing, and so may be greater than the opacity  $\kappa_e$  in the outer layers. This would help delay the  $^{56}\text{Ni}$  luminosity takeover.

The wavelength of the early emission depends on the photospheric radius,  $r_p$ , defined as the location where the optical depth  $\tau = \int_{r_p}^{\infty} \rho_f \kappa dr = 1$ , or

$$r_p = t^{(n-3)/(n-1)} \left( \frac{\zeta_\rho \kappa M v_t^{(n-3)}}{n-1} \right)^{1/(n-1)} \quad (24)$$

The effective temperature of the emission  $T_{\text{eff}} = (L_{c,\text{iso}}/4\pi r_p^2 \sigma)^{1/4}$  is then, for  $n = 10$

$$T_{\text{eff}} = 2.5 \times 10^4 a_{13}^{1/4} \kappa_e^{-35/36} t_{\text{day}}^{-37/72} \text{ K}. \quad (25)$$

At  $t = 1$  day, the emission peaks at wavelengths  $\lambda \approx 1000 \text{ \AA}$ , however the Rayleigh-Jeans tail of the blackbody extends into the near UV and optical.

While the analytic solution captures the essential physical effects, it neglects the ejecta asymmetry and non-radial transport. We have therefore calculated numerical light curves using a 3-D non-grey radiation transfer code which also accounts for the effects of line opacity and  $^{56}\text{Ni}$  heating (Kasen et al. 2006). For simplicity, we use an artificial ejecta model with density profile  $\rho_f(r, \theta, t) = \rho_0(r, t) f_0(\theta)$ , where the function  $f_0(\theta)$  now describes the angular structure of the conical hole region

$$f_0(\theta) = f_h + (1 - f_h) \frac{x^m}{1 + x^m} \left( 1 + A \exp \left[ -\frac{(x-1)^2}{(\theta_p/\theta_h)^2} \right] \right) \quad (26)$$

where  $x = \theta/\theta_h$ . This formula approximates the results of simulation in the homologous phase choosing  $m = 8$ ,  $f_h = 0.1$ ,  $\theta_h = 30^\circ$ ,  $\theta_p = 15^\circ$ , and  $A = 1.8$ . The pressure profile in the shocked region was taken from Eq. 18.

The light curve calculation (Figure 2) shows that the early collision luminosity is dramatic when the companion is a RG at  $a = 2 \times 10^{13} \text{ cm}$ . The numerical results agree with the analytic estimate (Eq. 22), and also illustrate the anisotropy of the radiation. The collision luminosity is brightest for viewing angles looking down upon the shocked region ( $\theta < \theta_h$ ), but a significant amount of radiation diffuses out at angles  $\theta \approx 90^\circ$ , and a few percent is even back-scattered along  $\theta \approx 180^\circ$ .

While the companion interaction produces a conspicuous signature (a kink) in the early bolometric light curve, most of the emission is in the UV; in the optical bands, the effect is less dramatic (Figure 3). For a RG companion, the B-band light curve shows a distinct bump at  $t < 5$  days which should be relatively easy to probe observationally. At redder wavelengths, or for smaller separation distance  $a$ , the collision simply modifies the shape of the light curve rise. However, because SN Ia light curves are quite standard, a statistical analysis of

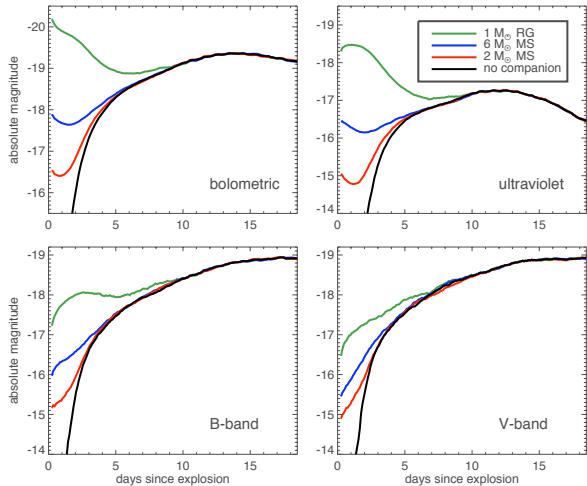


FIG. 3.— Signatures of companion interaction in the early broadband light curves of Type Ia supernovae. We model three different progenitor scenarios: a RG companion at  $a = 2 \times 10^{13}$  cm (green lines), a  $6 M_{\odot}$  MS companion at  $a = 2 \times 10^{12}$  cm (blue lines) and a  $2 M_{\odot}$  MS companion at  $a = 5 \times 10^{11}$  cm (red lines). The ultraviolet light curves are constructed by integrating the flux in the region 1000 – 3000 Å and converting to the AB magnitude system. For all light curves shown, the viewing angle is  $\theta = 0^{\circ}$ .

(good quality) early time photometry should be able to pull out these subtle differences.

### 5. OBSERVATIONAL PROSPECTS

The results derived here suggest a new means for constraining supernova companions using early photometric observations. Table 1 summarizes the analytic estimates of the collision emission for various SNe Ia progenitors. The theoretically predicted signatures appear to be quite robust, as they rely only on established physics familiar from the core collapse SNe context. However, further numerical studies using multi-dimensional radiation-hydrodynamical calculations (and including non-equilibrium effects) will be needed to refine the detailed light curve and spectrum predictions.

For all companion types, signatures of the collision will be prominent only for viewing angles looking down upon the shocked region, or  $\sim 10\%$  of the time. Detection will therefore require high cadence observations of many supernovae at the earliest phases ( $\lesssim 5$  days) and at the bluest wavelengths possible. Ironically, these observations may sometimes be easier for distant SNe. At redshifts  $z \gtrsim 0.5$ , the UV flux would be redshifted into the U-band, while cosmological time dilation would prolong the light curve by a factor  $(1+z)$ .

Detecting the collision signatures becomes significantly easier for larger separation distances. Current optical and UV data sets likely already constrain red giant companions ( $a \simeq 10^{13}$  cm). Ongoing or upcoming surveys could be tuned to probe the larger ( $M \gtrsim 3 M_{\odot}$ ) main sequence companions ( $a \simeq 10^{12}$  cm). Optical detection of the smallest  $\sim 1 M_{\odot}$  main sequence companions ( $a \simeq 10^{11}$  cm) will be challenging, requiring measurement of subtle differences in the light curves at  $t \lesssim 2$  day. However in all cases the prompt X-ray burst should be bright. Proposed X-ray surveys (e.g., EXIST, Grind-

lay 2005) may then detect a large number of collision bursts every year, at least in the case of MS companions which produce harder radiation. If non-equilibrium or non-thermal shock effects are operative, some hard radiation may accompany all bursts.

The most compelling reason for studying the collision emission is that it offers a straight-forward measure of the separation distance between the stars. This value can be determined from the duration of the X-ray burst ( $\Delta t_x \simeq a/v$ ), or its temperature (Eq. 7), or from the luminosity of the early optical/UV emission (Eq. 22). If we in turn assume that the companion is in Roche lobe overflow, its radius can be inferred  $R_{\star} \sim a/3 - a/2$ . In principle, the ratio  $a/R_{\star}$  itself could be constrained using a statistical sample of SNe Ia, as the anisotropy of the emission depends on the opening angle,  $\theta_h$ , of the shocked region of ejecta.

While our discussion has focused on Type Ia supernovae, similar signatures of companion interaction should apply to Type Ib/Ic and some Type II SNe which may arise from close massive binaries (Podsiadlowski et al. 1992). In these cases, the shock breakout from the exploding star will contribute to the luminosity on comparable timescales, likely producing two peaks in the X-ray emission. Some gamma-ray bursts might also come from binary systems, and the interaction of the relativistic material with a stellar companion may produce another type of X-ray flare (MacFadyen et al. 2005).

It is also possible that early emission from SNe stems from a collision not with the companion star, but with a surrounding circumstellar medium (CSM). To substantially decelerate the ejecta, the CSM would need to have a mass  $\sim 0.01 - 0.1 M_{\odot}$  located at radii  $\sim 10^{11} - 10^{13}$  cm. A slow ( $10 \text{ km s}^{-1}$ ) stellar wind moves beyond these distances is less than a year, so it may be difficult to realize these conditions in a single degenerate scenario of SNe Ia. In the double degenerate merger scenario, the total mass of the system can exceed  $M_{\text{ch}}$ , and a few  $0.1 M_{\odot}$  of excess carbon/oxygen may linger in the vicinity. If this material remains at the tidal radius  $\sim 10^9$  cm, the resulting emission will be extremely brief ( $\sim 1$  sec), however if some mass is puffed out to larger radii in the super-Eddington accretion phase of the merger, the emission may be similar to that discussed here. Interaction with a spherical CSM is distinguishable from companion interaction by its luminosity function; in the former case, the emission should be nearly the same from all viewing angles.

In either case, the early time emission of supernovae provides much needed insight into the nature of the progenitor system. Observational surveys could be designed, either from space or the ground, to acquire the collision signatures in a systematic way. If one collects a significant number of events, it will be possible to correlate the measured separation distances with the properties of the ordinary  $^{56}\text{Ni}$  powered light curve and spectra. Such observations would provide direct, empirical insight into how the parameters of the progenitor system influence the outcome of supernova explosions.

The author is grateful for comments from E. Ramirez-Ruiz, T. Plewa, S.E Woosley, and the referee C. Matzner. Support was provided by NASA through Hubble fellowship grant #HST-HF-01208.01-A awarded by the Space

TABLE 1  
 PROPERTIES OF TYPE IA SUPERNOVA COLLISION EMISSION - ANALYTIC ESTIMATES

Companion	a	$E_x$	$\Delta t_x$	$L_{x,iso}$	$T_x$	$L_{c,iso}$ (1 day)	$t_c$
RG ( $M \sim 1 M_\odot$ )	$2 \times 10^{13}$ cm	$3.9 \times 10^{47}$ ergs	1.9 hours	$5.8 \times 10^{44}$	0.07 keV	$2 \times 10^{43}$	9.6 days
MS ( $M \sim 6 M_\odot$ )	$2 \times 10^{12}$ cm	$3.9 \times 10^{46}$ ergs	11 mins	$5.8 \times 10^{44}$	0.2 keV	$2 \times 10^{42}$	3.8 days
MS ( $M \sim 2 M_\odot$ )	$5 \times 10^{11}$ cm	$9.6 \times 10^{45}$ ergs	2.8 mins	$5.8 \times 10^{44}$	1.0 keV	$5 \times 10^{41}$	2.2 days
MS ( $M \sim 1 M_\odot$ )	$3 \times 10^{11}$ cm	$5.8 \times 10^{45}$ ergs	1.7 mins	$5.8 \times 10^{44}$	1.4 keV	$3 \times 10^{41}$	1.8 days

Telescope Science Institute, which is operated by the Association of Universities for Research in Astronomy, Inc., for NASA, under contract NAS 5-26555. This re-

search has been supported by the DOE SciDAC Program (DE-FC02-06ER41438). Computing time was provided by ORNL through an INCITE award and by NERSC.

## REFERENCES

- Arnett, W. D. 1982, ApJ, 253, 785  
 Arnett, W. D., Bahcall, J. N., Kirshner, R. P., & Woosley, S. E. 1989, ARA&A, 27, 629  
 Ballantyne, D. R., & Ramirez-Ruiz, E. 2001, ApJ, 559, L83  
 Branch, D., Livio, M., Yungelson, L. R., Boffi, F. R., & Baron, E. 1995, PASP, 107, 1019  
 Chevalier, R. A. 1992, ApJ, 394, 599  
 Chevalier, R. A., & Soker, N. 1989, ApJ, 341, 867  
 Chugai, N. N. 1986, Soviet Astronomy, 30, 563  
 Cid-Fernandes, R., Plewa, T., Rózycka, M., Franco, J., Terlevich, R., Tenorio-Tagle, G., & Miller, W. 1996, MNRAS, 283, 419  
 Fryxell, B. et al. 2000, ApJS, 131, 273  
 Fryxell, B. A., & Arnett, W. D. 1981, ApJ, 243, 994  
 Grindlay, J. E. 2005, New Astronomy Review, 49, 436  
 Hachisu, I., Kato, M., & Nomoto, K. 1996, ApJ, 470, L97+  
 Kasen, D., Nugent, P., Thomas, R. C., & Wang, L. 2004, ApJ, 610, 876  
 Kasen, D., Roepke, F., & Woosley, S. 2009, Nature Accepted  
 Kasen, D., Thomas, R. C., & Nugent, P. 2006, ApJ, 651, 366  
 Katz, B., Budnik, R., & Waxman, E. 2009, ArXiv e-prints  
 Kerzendorf, W. E., Schmidt, B. P., Asplund, M., Nomoto, K., Podsiadlowski, P., Frebel, A., Fesen, R. A., & Yong, D. 2009, ArXiv e-prints  
 Klein, R. I., & Chevalier, R. A. 1978, ApJ, 223, L109  
 Leonard, D. C. 2007, ApJ, 670, 1275  
 Livne, E., Tuchman, Y., & Wheeler, J. C. 1992, ApJ, 399, 665  
 MacFadyen, A. I., Ramirez-Ruiz, E., & Zhang, W. 2005, arXiv:astro-ph/0510192  
 Maoz, D., & Mannucci, F. 2008, MNRAS, 388, 421  
 Marietta, E., Burrows, A., & Fryxell, B. 2000, ApJS, 128, 615  
 Mattila, S., Lundqvist, P., Sollerman, J., Kozma, C., Baron, E., Fransson, C., Leibundgut, B., & Nomoto, K. 2005, A&A, 443, 649  
 Matzner, C. D., & McKee, C. F. 1999, ApJ, 510, 379  
 Modjaz, M., et al. 2009, ApJ, 702, 226  
 Pakmor, R., Röpke, F. K., Weiss, A., & Hillebrandt, W. 2008, A&A, 489, 943  
 Podsiadlowski, P., Joss, P. C., & Hsu, J. J. L. 1992, ApJ, 391, 246  
 Ruiz-Lapuente, P. et al. 2004, Nature, 431, 1069  
 Soderberg, A. M. et al. 2008, Nature, 453, 469  
 Wang, L., & Wheeler, J. C. 2008, ARA&A, 46, 433  
 Weaver, T. A. 1976, ApJS, 32, 233  
 Wheeler, J. C. et al. 1993, ApJ, 417, L71+  
 Wheeler, J. C., Lecar, M., & McKee, C. F. 1975, ApJ, 200, 145  
 Zel'Dovich, Y. B., & Raizer, Y. P. 1967, Physics of shock waves and high-temperature hydrodynamic phenomena